島根大学地球科学研究報告　37, 1～10 ページ（2020 年 3 月）
Earth Science Rept. Shimane Univ., 37, p.1～10（2020）

Article

Petrology and mineral chemistry of the Karasugasen lava dome and associated pyroclastic flow deposits

Yutaka Ito*, Andreas Auer*

Abstract

The Karasugasen lava dome is part of the Daisen – Hiruzen Volcanic complex and was the source of a large number of Block and Ash flows. Products directly overlie the Aira Tanzawa tephra (AT), and the majority of erupted material is preserved in three voluminous lobes to the south and southeast of Mt Daisen. Dacitic magmas with adakitic characteristics were sourced from a large magma chamber in the shallow crust crystallizing between 4 and 12 km depth, at temperatures between 803 and 920 °C and oxygen fugacities of Δlog +1.7 to +1.8 above the NNO buffer. Cores of magnesium rich orthopyroxene phenocrysts are not in equilibrium with the host dacite and may be a rare evidence for insipient mafic replenishment of the voluminous magma chamber beneath the Daisen Volcanic complex.

Key words: Daisen Volcano, Karasugasen Lava Dome, Sasaganaru Block and Ash flows, Thermobarometry

Introduction

Magmas of arc volcanoes are often stored at shallow crustal levels at depths between 3 and 15 km prior to eruption (Sparks and Young 2002; Annen *et al*., 2008; Auer *et al*., 2015, 2016). Direct evidence for the existence of shallow magma chambers can be found by monitoring volcanic earthquakes, passive seismic records, ground deformation and gas emissions (Sparks and Cashman 2017). These methods are also at the core of modern volcanological observatories, dedicated to warning and prevention of volcanic hazards in communities around active volcanoes and to aviation. In addition, the volatile contents of phenocryst-hosted melt inclusions, variations in mineral chemistry as well as experimental work can help to decipher ascent and storage conditions of magma in active volcanic systems (Cashman and Sparks 2013). The detailed structure of magma storage systems and the processes within them, during periods of quiescence and unrest, are key to the understanding of timing and style of past and forthcoming eruptions (Nakagawa *et al*., 2011). Conceptual models of shallow crustal magma chambers range from simple liquid spheres within the crust, which are transiently emptied during eruption and replenished from depth, to complex trans-crustal mush columns with several distinct magma reservoirs, that can be tapped during an eruptive episode (Nakagawa *et al*., 1999; Auer *et al*., 2013; Cashman *et al*., 2017). One of the fundamental tasks is, to characterize the composition and physical conditions (P,T, fO_2) under which magma was stored before an eruption.

Karasugasen in one of the young lava domes of Mt. Daisen which has recently been subject of several detailed stratigraphic and petrological studies (Kimura *et al*., 2005; Yamamoto 2017). However, no detailed glass and mineral analytic of the erupted products has been done so far. Here we present a comprehensive characterization of petrography, glass and mineral chemistry to constrain the magma plumbing system and pre-eruptive magma storage conditions at Karasugasen lava dome.

Geological Background

The Karasugasen lava dome is part of Mt Daisen, a large stratovolcano located in the San-in district, southwest Japan (Fig. 1). Volcanism in this area is related to the subduction of the Philippine Sea Plate (Kimura *et al*., 2014). Magmas of Mt. Daisen have been identified as adakites, their origin interpreted as a result of slab melting (Morris 1995; Feineman *et al*., 2013; Pineda-Velasco *et al*., 2018). The volcanic products are mostly dacite dome lavas, block and ash flows and Plinian tephras (Tsukui 1984, 1985). Karasugasen is one of the eruptive centers of Daisen-Hiruzen volcano group which was active from 1 Ma to 17 ka (Tsukui 1984; Yamamoto 2017). Products of the Karasugasen lavadome directly overly the Aira Tanzawa Tephra (Fig. 2b) which gives a minimum age constrain of 30,009±189 ka cal. yrs BP (Smith *et al*., 2013). Deposits have been subdivided into several subunits, which are the Sasaganaru ash fall deposit (SaA - equivalent to the Shitanohoki (Sh) in the stratigraphy of Okada nad Ishiga (2000)). SaA is overlain by several large flow units derived from dome collapse events at the main Karasugasen lavadome, collectively termed the Sasaganaru pyroclastic flows (SaF). Kimura *et al*. (2005) subdivided these block and ash flow deposits into 9 subunits mainly based on characteristics of essential components such a vesicularity and state of oxidation (Fig. 2a). These deposits are largely confined to 3 valleys in the south and southeast of Daisen (Miyou lobe to

* Department of Geoscience, Shimane University; 1060 Nishikawatsu, Matsue, 690-8504, Japan

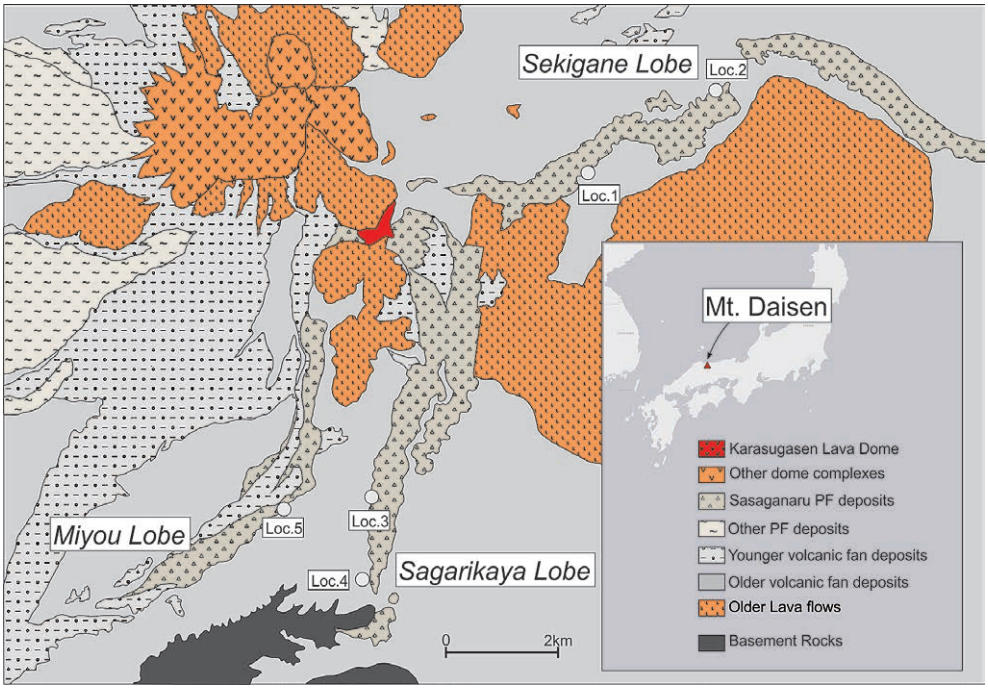

Fig. 1. Geological map of Karasugasen lava dome and associated products, in San-in district, southwest Japan. The Sasaganaru pyroclastic flow deposits (Triangular dots) are preserved as three distinct lobes along valleys in the southern and southeastern sector of the mountain. Each lobe area is around 2 × 7 km^2. Five sampling positions of the representative outcrops are plotted in the map.

the southwest, Sagarikaya lobe to the south, and Sekigane lobe to the east) which show characteristic "shoestring morphology" (Fig. 1). A distal correlative of the SaF is the Odori ashfall (Fig. 2b). SaF and Odari ashfall are overlain by Higashidaisen Vulcanian eruption sequence (HgA) and the Higashidaisen Pumice (HgP) (Fig. 2a, b)

Methods

Field investigations were done during May 2018 and July 2019. Profile sections were drawn and we were able to reconstruct and follow the stratigraphy established by Kimura *et al*. (2005). Juvenile pyroclastic rocks were collected from several units for subsequent geochemical and mineral analyses. Whole rock composition of 7 samples was analysed by X-ray fluorescence spectrometry (XRF) using the Rigaku Co. Ltd. RIX-2000 spectrometer at Shimane University. Samples were washed and cut into small chips of 1.5 cm size to remove altered domains or weathered rinds. Subsequently, samples were crushed into fine powder using a tungsten carbide ring mill with crushing times of 90 seconds. About 2.5 g (maximum error 0.1 g plus) of the powdered sample was put in a small pot of about 12 g using an electronic balance. The sample is then placed in a muffle furnace set at 900 degrees for 1 hour to determine loss on ignition (LOI). Fused disks were prepared with a flux to the sample ratio of 2:1, the flux used was a mixture of $LiBO_2$ and $Li_2B_4O_7$ in a ratio of 8:2. Thinsections were prepared from several units of pyroclastic flow deposits originating from the Karasugasen lava dome collected during field surveys. These samples are first selected from the core portion of the sample in order to remove the weathered portion, and a chip having a length of 2 cm, a width of 4 cm and a thickness of about 5 mm is prepared. Since the sample to be handled are relatively brittle we vacuum impregnated them before preparing polished slides. Mineral and glass analysis were done on an EPMA (JEOL 8530F) at Shimane University with operation conditions of 15 kv acceleration voltage and 20 nA beam current and a focussed electron beam for minerals and a defocussed beam for glass measurements. Counting times were 10 seconds (peak) and 5 seconds (background) except for FeO and MgO in plagioclase (120/40 s) and Cr_2O_3 in pyroxene (60/30 s). The results were monitored using Smithsonian mineral standards.

Results

Glass and Whole rock composition

Juvenile blocks from the Sasaganaru pyroclastic flows are generally highly porphyritic with variable vesicularity and different degrees of oxidation. Pyrogenic minerals include plagioclase, amphibole, orthopyroxene, Fe-Ti oxides and biotite (Fig. 2c).

Results from geochemical analysis generally agree well with those obtained during earlier studies (Kimura *et al*., 2005; Yamamoto and Hoang 2019). All samples are medium K dacites (Fig. 3) which show typical adakitic character. Results from whole rock analysis are shown in Table 1

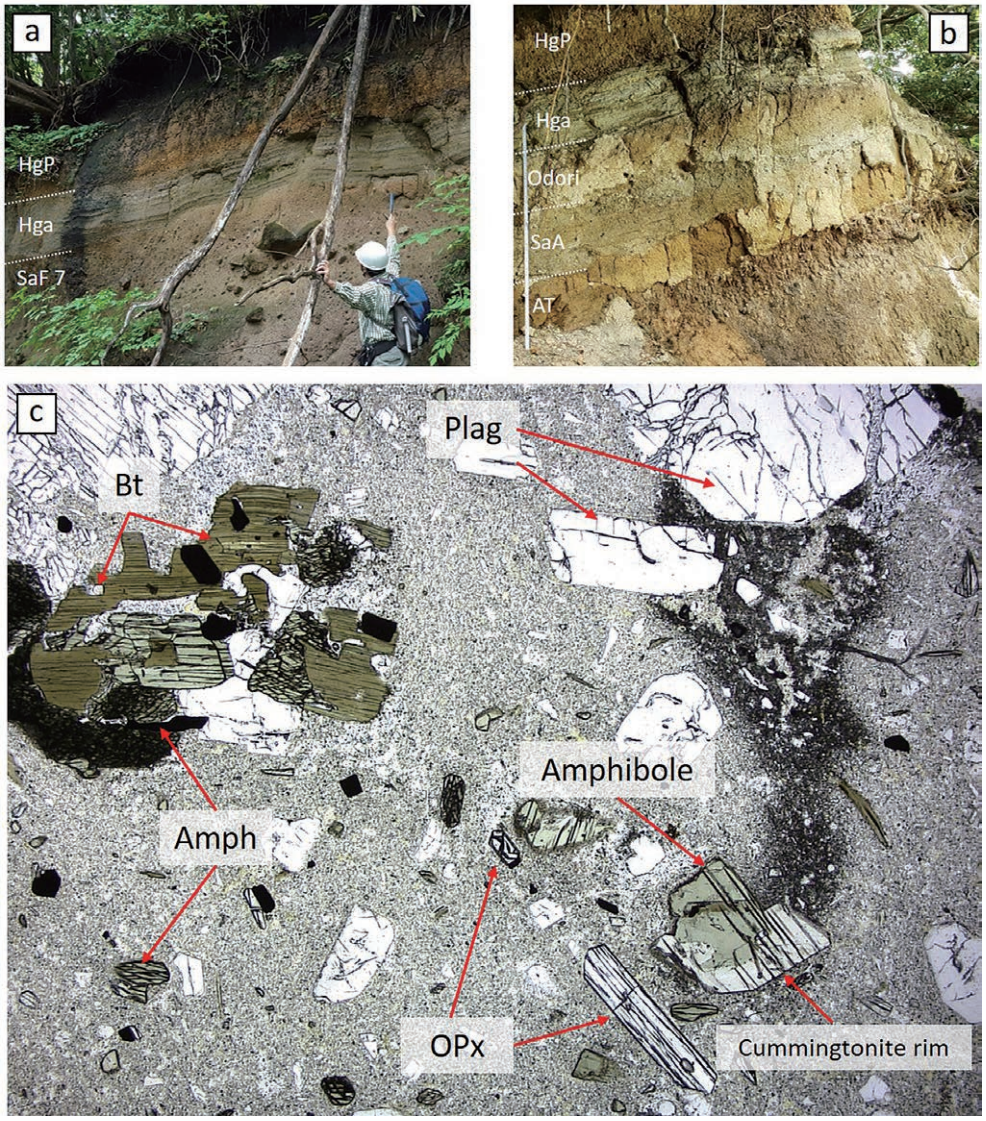

Fig. 2. (a) Sasaganaru Pyroclastic flow deposits and associated overlaying tephra's Higashi Daisen Ash (HgA) and Higashidaisen Pumice (HgP) in a proximal location. (b) At distal locations, products from Karasugasen, ca be resolved into a lower Sasaganaru Ash (SaA) and the Odori ash fall deposit, corellative to SaF. Both are overlaying the Aira tanzawa tephra. (c) Major constituent minerals in the SaF deposits are plagioclase, amphibolite, pyroxene, biotite, and Fe-Ti oxide and rare cummingtonite.

and plotted in Fig. 3. Groundmass glass composition is exclusively rhyolitic. Whole rock composition as well as matrix glass compositions have been used for equilibrium testing with phenocryst phases (see below).

Mineral composition, zoning patterns and reaction textures

Plagioclase

Plagioclase is the dominant phenocryst and groundmass phase in all the samples (Fig. 4a, b). Modal proportion ranges from 25 to 28%, and maximum crystal length is 1 cm. Both homogenous and oscillatory zoned euhedral phenocrysts are common in all samples. Some plagioclase show resorption textures and subsequent overgrowth (Fig. 4b). Some of plagioclase hosts smaller crystals of amphibole. Plagioclase was divided into three textural groups, which are: phenocryst, glomeroporphyritic aggregates and groundmass microphenocryst. Compositional variation ranges from An30 to An 65 and some representative compositions are given in Table 2.

Amphibole

Amphibole occurs as euhedral crystals up to 5 mm in size (Fig. 4c, d, e). Modal proportion varies between 8.1 and 9.3%. Several distinct textural types have been identified which are: Homogeneous amphibole, zoned amphibole, amphibole poikilitically enclosing Fe-Ti oxide phases and, resorbed amphibole which show signs of remelting. Some amphiboles show strong alumina enrichment in their outer rims (Fig. 4c), others show alumina rich cores (Fig. 4d). In addition, many amphiboles show breakdown rims of variable thickness. Amphibole are classified as tschermakite

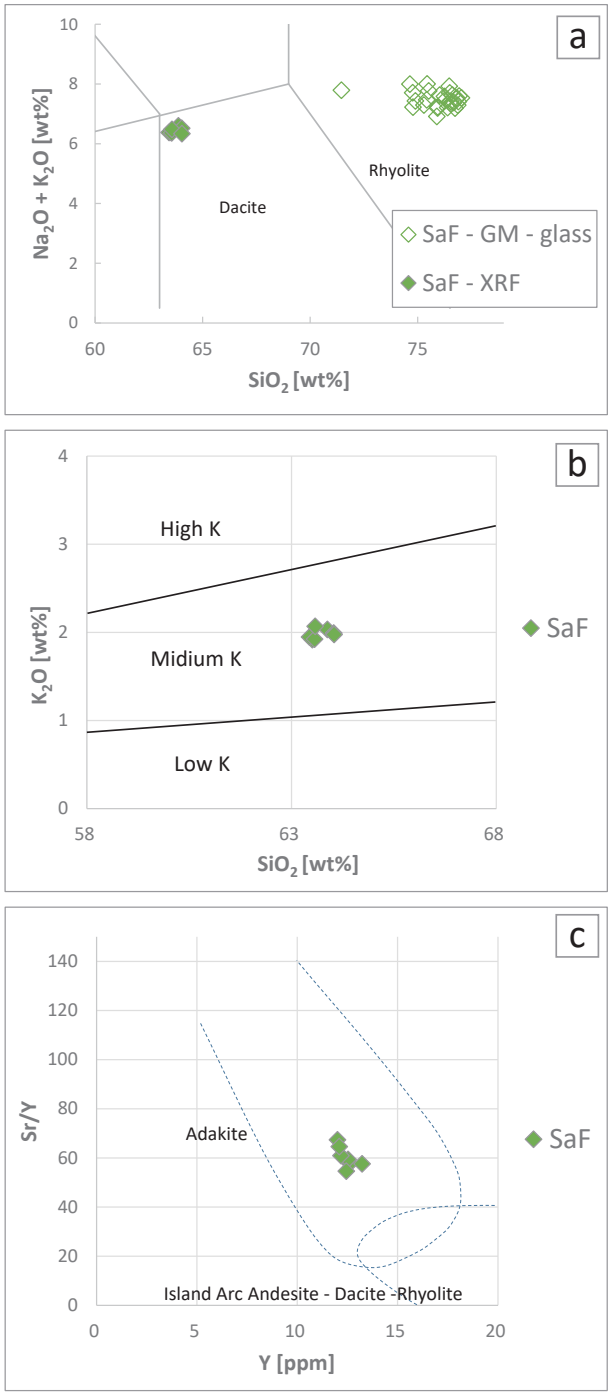

Fig. 3. (a, b), Classification of SaF Matrix-glass and whole-rock compositions, using the TAS diagram and the SiO2 – K2O discrimination diagram. (c) Trace element variation diagram (Y-Sr/Y) composition shows, that products from Karasugasen are Adakites.

and magnesio-hornblende, following the system of Leake *et al*. (1997). Some representative compositions are given in Table 2. Rims of cummingtonite are occasionally found on some of the amphiboles (Fig. 2c).

Orthopyroxene

Orthopyroxene occurs as euhedral phenocrysts up to 1 mm in size (Fig. 4f). Modal proportion varies between 1.5 and 2.2 %. Pleochroism varies from colorless to light yellow. The diameter can reach up to 1 mm at the maximum. The majority of orthopyroxene shows magnesium numbers between Mg#65- Mg#68. However, as small population of orthopyroxene shows cores with much a higher magnesium concentration of around Mg#83 (Fig. 4g). Some representative compositions are given in Table 2 .

Fe-Ti Oxides and Biotite

Fe-Ti oxides occur as small euhedral crystals with cubic or rhombohedral shapes. Modal proportion varies between 1.8 and 2.5 %. The diameter is as small as about 0.1 mm. Fe-Ti oxides also occur within plagioclase, hornblende and orthopyroxene. Representative ilmenite and magnetite compositions are given in Table 2. Biotite occurs as euhdral or subhedral crystals (Fig. 4h). Modal proportion varies between 0.8 and 1 %. The diameter is about 1-2 mm. Similar to amphibole, biotite rims often show breakdown textures of variable size. Some representative compositions are given in Table 2.

Discussion - Erupted magma and its storage conditions

The majority of erupted magmas from Daisen volcano are dacites and a few subordinate andesitic and basaltic lava flows (Feineman *et al*., 2013). Products from the upper tephra group of Mt Daisen are exclusively highly evolved dacites (Yamamoto and Hoang 2019). Some coeval mafic rocks exist in the Daisen Hiruzen complex but trace element characteristics are variably interpreted either to support them as parental melts of the dacites (Tamura *et al*., 2000, 2003; Zellmer *et al*., 2012) or to preclude a genetic relationship between these mafic rocks and the evolved felsic magmas (Feineman *et al*., 2013; Kimura *et al*., 2014; Pineda-Velasco *et al*., 2018). In fact, Pineda-Velasco *et al*. (2018) suggest that andesitic and dacitic compositions at Daisen volcano are directly derived from the subducted slab (+sediment component / infiltrated mantle component). Their proposed model completely lacks the ubiquitous transient mafic replenishment that has been proposed for many arc volcanoes. Instead evolved melts reach the crust in “ready made” diapirs and form “big tank” type of magma chambers (Glazner *et al*., 2004). A large number of recent studies has argued against such magma chambers, favouring growth of upper crustal magma storage by incremental addition of mafic melt (Annen *et al*., 2015). However, evidence for mafic melts is sparse in the products of young Daisen tephras.

We calculated temperature, pressure, water content, and oxygen fugacity of the magma using amphibole composition (Ridolfi *et al*., 2010). Amphibole barometry yields pressures between 116 and 713 MPa, however, the majority of amphiboles clusters around pressures of 200 MPa. Significantly higher pressures are calculated for a number of alumina rich amphibole, but textures preclude

Table 1. Representative whole-rock composition.

[wt%] / Sample	SaF-1	SaF-2	SaF-3	SaF-4	SaF-5	SaF-6	SaF-7
SiO_2	63.51	63.44	63.88	63.56	64.03	63.58	64.04
TiO_2	0.41	0.40	0.43	0.40	0.44	0.45	0.43
Al_2O_3	17.15	17.17	17.60	17.55	17.52	17.22	17.09
FeO	3.77	3.71	3.81	3.71	3.85	3.97	3.93
MnO	0.07	0.07	0.06	0.07	0.07	0.07	0.07
MgO	1.75	1.71	1.73	1.68	1.78	1.89	1.81
CaO	4.69	4.67	4.73	4.64	4.73	4.46	4.28
Na_2O	4.47	4.43	4.56	4.44	4.52	4.41	4.36
K_2O	1.92	1.95	2.03	1.92	1.99	2.07	1.98
P_2O_5	0.14	0.15	0.18	0.14	0.18	0.18	0.15
LOI	0.95	1.38	0.13	1.15	0.15	0.83	0.96
Total	98.82	99.08	99.15	99.27	99.27	99.13	99.10
[ppm]							
Ba	373	370	368	376	383	392	396
Ce	33.0	31.9	38.8	35.2	37.1	34.8	30.4
Cr	9.98	11.93	13.60	11.65	8.22	7.85	13.79
Ga	17.3	19.4	19.8	20.1	19.4	18.9	19.4
Nb	7.26	7.63	10.72	7.26	9.73	10.22	7.51
Ni	8.54	8.63	10.50	9.10	11.15	11.80	10.40
Pb	8.62	9.71	7.09	10.36	7.75	8.95	8.73
Rb	53.2	52.8	46.0	50.0	46.6	53.2	49.9
Sr	729	745	809	743	782	763	680
Th	9.33	3.44	4.14	3.44	4.71	5.52	5.06
V	53.2	54.8	61.8	61.0	63.4	64.2	57.1
Y	12.6	12.5	12.0	12.2	12.1	13.2	12.4
Zr	173	170	186	173	185	181	168

a simple interpretation, because these amphiboles occur as phenocryst cores as well as phenocryst rims (Fig. 4c, d). It is conceivable, that such compositional variation is rather an effect of variable temperature than pressure as was previously demonstrated by Erdmann *et al*. (2014). To better constrain pre-eruptive magma storage, we also applied orthopyroxene – liquid thermobarometry (Putirka 2008), yielding crystallization conditions between 0 and 300 MPa and 840 to 870 ˚C. Fe-Ti oxide composition was also used to put additional constrain on magma temperature and oxygen fugacity showing values of between 838 to 898 ˚C and Δlog +1.0 to +2.2 respective to the nickel-nickel oxide buffer (Lepage 2003). The Plagioclase-melt hygrometer was applied to constrain melt water contents (Lange *et al*., 2009) which determined melt water contents between 5.2 and 7.1 wt% H_2O (Fig. 5b).

Many arc volcanoes, similar to Mt Daisen (e.g. Mt St. Helens or Mt Pinatubo) are characterized by voluminous, long living shallow dacitic magma chambers. In some cases, their bimodal nature and a direct genetic link to mafic parental compositions can be found directly within the erupted dacites such in the form of basaltic enclaves, relict olivine or melt inclusions of basaltic composition (Churikova *et al*., 2013; Auer *et al*., 2018). In other cases – like at Mt Daisen – such direct evidence for mafic replenishment of the shallow magmatic system seems to be completely missing. Besides petrological evidence, disequilibrium textures and mineral zonation can also sometimes reveal cryptic mafic replenishment and magma ascent processes through magmatic plumbing systems. Mg-rich orthopyroxenes, might be a rare clue to such mafic melts at Mt Daisen. Similar compositions had previously been described by Tamura *et al*. (2003) – see their figure 5d and have also been found in the Sasaganaru pyroclastic flow deposits.

Such orthopyroxenes would not be in equilibrium with any product from the Younger tephra group, but possibly with some of the older basalts at Daisen (Fig. 6). We speculate that the presence of these high-Mg pyroxenes provide a rare clue to mafic magma recharge at Mt Daisen.

Conclusion

The Karasugasen lava dome was source for a large number of Block and Ash flows, distributed in three voluminous

Table 2. Representative Mineral compositions.

Ph: Phebocrysts, Gm: groundmass, C: core, R: Rim

Sample	Plagioclase			Amphibole			Orthopyroxene			Fe-Ti oxide			Biotite			Glass	
Number	SaF-7p_5	SaF-7p_62		SaF-5_1	SaF-6_1		SaF-7pb_1	SaF-7pa_9		SaF-7_1	SaF-7_2		SaF-4_12	SaF-7p_3		SaF-4_6	SaF-4_11
Type	Gm	Ph-R		Ph-R	Ph-R		Ph-R	Ph-C		Ph-R	Ph-R		Ph-R	Ph-R		Gm	Gm
SiO_2	55.97	52.03		43.20	43.39		53.53	54.82		0.06	0.02		37.29	36.55		74.77	77.03
TiO_2	0.00	0.01		2.01	1.92		0.07	0.12		5.24	33.53		3.37	3.01		0.18	0.23
Al_2O_3	27.56	30.33		12.50	12.46		0.59	2.08		2.25	0.35		15.34	14.99		13.30	10.85
Cr_2O_3	0.00	0.00		0.00	0.00		0.00	0.36		0.07	0.03		—	—		—	—
FeO	0.27	0.36		9.35	10.16		20.48	9.76		84.54	59.80		13.18	17.17		0.73	1.18
MnO	0.02	0.00		0.12	0.09		0.71	0.18		0.33	0.26		0.06	0.24		0.04	0.03
MgO	0.02	0.01		16.30	15.79		24.29	31.20		1.44	1.73		15.95	13.29		0.06	0.38
CaO	9.31	12.61		10.30	10.74		0.46	1.12		0.00	0.00		0.02	0.03		0.93	0.20
Na_2O	5.92	4.01		2.34	2.38		0.01	0.04		—	—		1.04	0.39		3.56	2.49
K_2O	0.22	0.12		0.71	0.63		0.00	0.00		—	—		8.17	8.82		4.15	5.04
ZnO	—	—		—	—		—	—		0.12	0.04		—	—		—	—
Cl	—	—		—	—		—	—		—	—		0.17	0.11		0.07	0.19
Total	99.30	99.48		96.83	97.55		100.13	99.68		94.03	95.77		94.57	94.59		97.77	97.63
Si	2.53	2.37		6.13	6.16		1.97	1.93		0.00	0.00		5.55	5.56	**Na_2O+K_2O**	**7.71**	**7.54**
Ti	0.00	0.00		0.21	0.20		0.00	0.00		0.31	0.62		0.38	0.34			
Al	1.47	1.63		2.09	2.08		0.03	0.09		0.10	0.01		2.69	2.69			
Cr	0.00	0.00		0.00	0.00		0.00	0.01		0.00	0.00		—	—			
Fe[III]	0.00	0.00		1.11	1.16		0.60	0.24		1.28	0.75		—	—			
Fe[II]	0.01	0.01		0.00	0.04		0.03	0.04		1.24	0.58		1.64	2.19			
Mn	0.00	0.00		0.01	0.01		0.02	0.01		0.01	0.00		0.01	0.03			
Mg	0.00	0.00		3.45	3.34		1.34	1.64		0.06	0.03		3.54	3.02			
Ca	0.45	0.62		1.57	1.63		0.02	0.04		0.00	0.00		0.00	0.01			
Na	0.52	0.35		0.64	0.66		0.00	0.00		0.00	0.00		0.30	0.11			
K	0.01	0.01		0.13	0.11		0.00	0.00		0.00	0.00		1.55	1.71			
Zn	0.00	0.00		—	—		—	—		0.00	0.00		—	—			
Cl	—	—		—	—		—	—		—	—		0.00	0.00			
Total	4.999	4.993		15.338	15.401		4.011	4.015		3.002	2.001		15.654	15.661			
An	**45.9**	**63.1**				**En**	**66.6**	**83.1**									
Ab	**52.8**	**36.2**	**Mg/Mg+Fe(II)**	**1.00**	**0.99**	**Fs**	**32.5**	**14.8**									

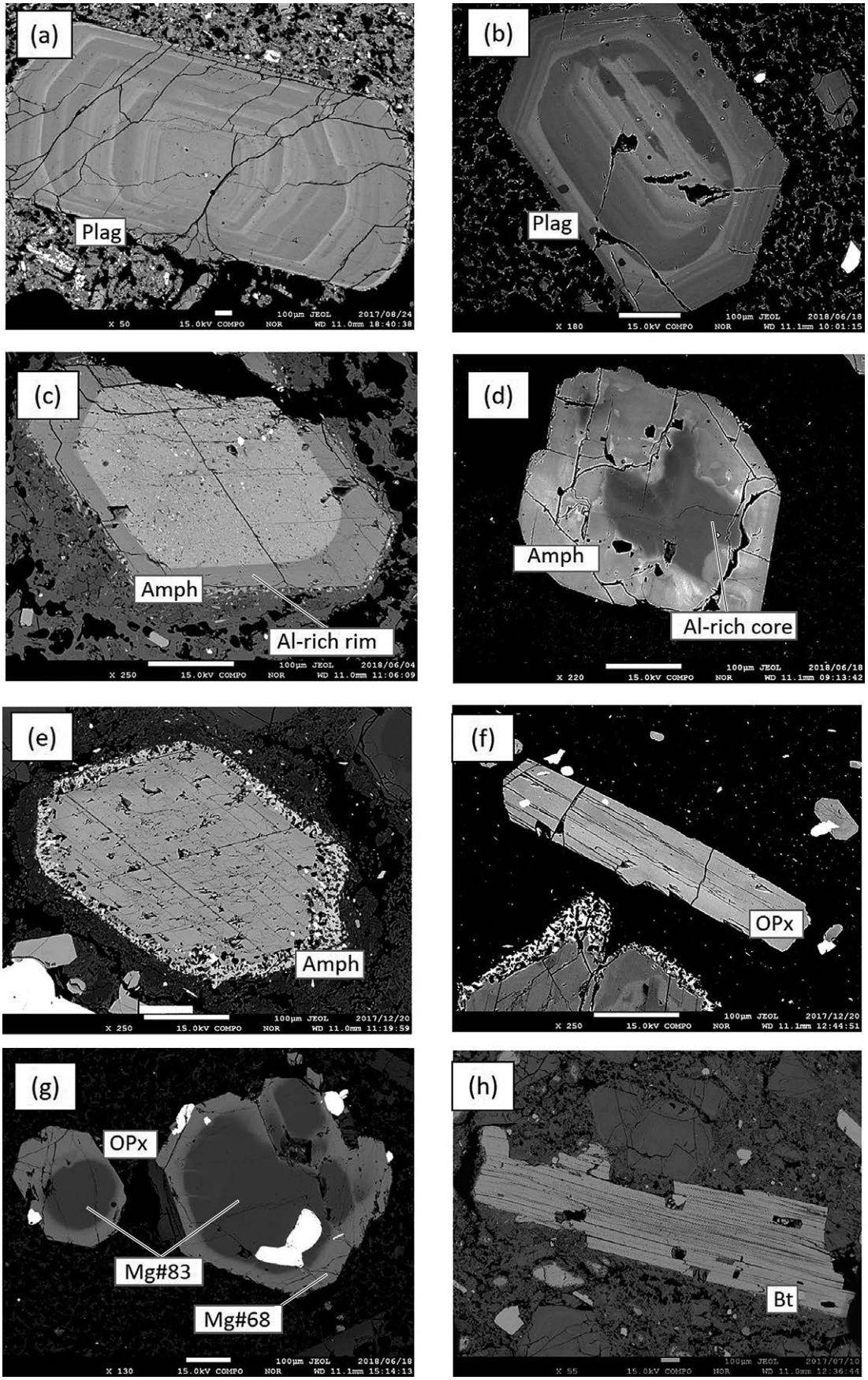

Fig. 4. Back scatter Electron Images (BEI) of (a) Oscillatory zoned plagioclase, (b) Normal zoned plagioclase with a strongly resorbed core, (c, d) Amphibole with Al-rich rim and core, respectively (e) Amphibole with a ca 30 μm wide breakdown rim, (f) Groundmass orthopyroxene, (g) Orthopyroxene phenocrysts with high Mg cores, (h) Groundmass Biotite

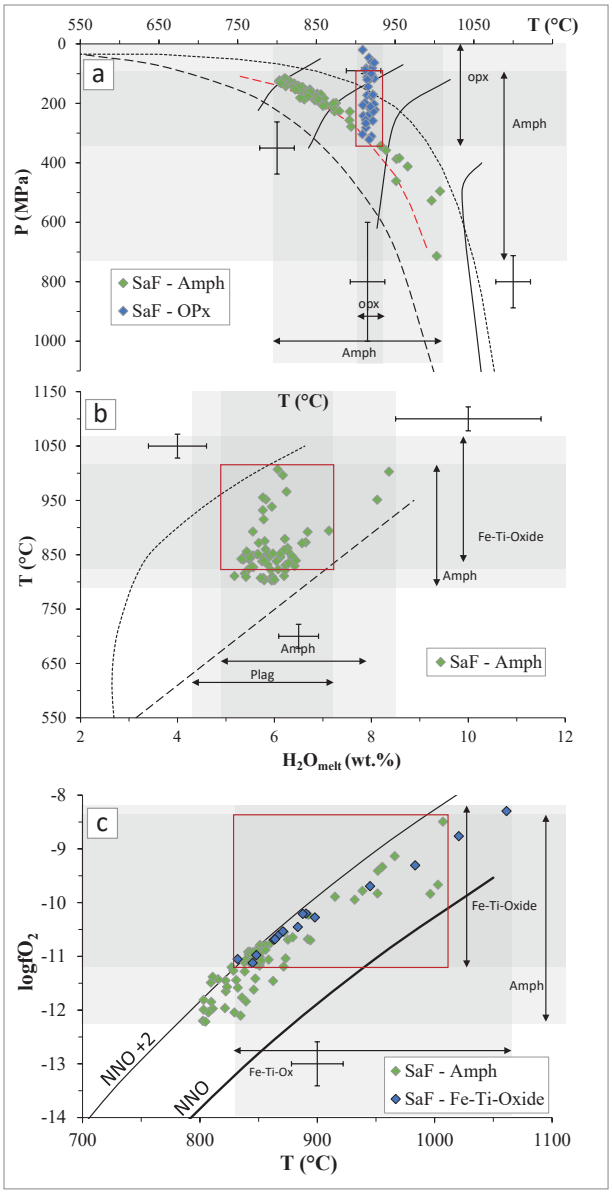

Fig. 5. Estimated pre-eruptive magma storage conditions based on (a) amphibole and orthopyroxene – liquid thermobarometry (b) Amphibole and plagioclase hygrometry (c) Amphibole and Fe-Ti-Oxide thermometry. Overlapping ranges of the respective methods are shown by red outlined squares.

lobes mainly to the south and southeast of Mt Daisen. Adacitic magmas of dacitic composition were sourced from a large magma chamber in the shallow crust crystallizing between 4 and 12 km depth (overlapping range between amphibole and orthopyroxene thermobarometry = 116 and 320 MPa) at temperatures between 803 and 920 °C and oxygen fugacities of Δlog + 1.7 to + 1.8 above the NNO buffer. Cores of magnesium rich orthopyroxene phenocrysts may be a rare evidence for insipient mafic replenishment of the voluminous magma chamber beneath the Daisen Volcanic complex.

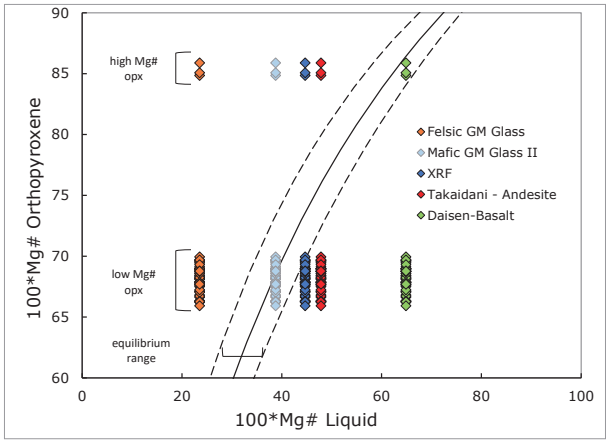

Fig. 6. Rhodes diagram plot, to test for equilibrium between orthopyroxene and liquid. Most orthopyroxenes are not in equilibrium with the most felsic groundmass glass compositions or the whole rock composition, but roughly in equilibrium with more mafic groundmass glass. The high Mg# orthopyroxene cores are not in equilibrium with any of the SaF products, but would be roughly in equilibrium with older Daisen basalts (Data for Takadani Andesite and Daisen basalt from Feinemann *et al*., 2013)

Acknowledgments

We would like to express our gratitude to Dr A. Kamei for his advice and support during the XRF analysis.

References

Annen C, Blundy JD, Leuthold J, Sparks RSJ (2015) Construction and evolution of igneous bodies: Towards an integrated perspective of crustal magmatism. *Lithos*, **230**, 206–221.

Annen C, Pichavant M, Bachmann O, Burgisser A (2008) Conditions for the growth of a long-lived shallow crustal magma chamber below Mount Pelee volcano (Martinique, Lesser Antilles Arc). *J Geophys Res Solid Earth*, **113**:

Auer A, Belousov A, Belousova M (2018) Deposits, petrology and mechanism of the 2010–2013 eruption of Kizimen volcano in Kamchatka, Russia. *Bull Volcanol*, **80**, 33.

Auer A, Martin CE, Palin JM, *et al.* (2015) The evolution of hydrous magmas in the Tongariro Volcanic Centre: the 10 ka Pahoka-Mangamate eruptions. *N Z J Geol Geophys*, **58**, 364–384. https://doi.org/10.1080/00288306.2015.1089913

Auer A, White JDL, Nakagawa M, Rosenberg MD (2013) Petrological record from young Ruapehu eruptions in the 4.5 ka Kiwikiwi Formation, Whangaehu Gorge, New Zealand. *N Z J Geol Geophys*, **56**, 121–133.

Auer A, White JDL, Tobin MJ (2016) Variable H_2O content in magmas from the Tongariro Volcanic Centre and its relation to crustal storage and magma ascent. *J Volcanol Geotherm Res*, **325**, 203–210. https://doi.org/10.1016/j.jvolgeores.2016.06.021

Cashman KV, Sparks RSJ (2013) How volcanoes work: A 25 year perspective. GSA Bull, **125**, 664–690.

Cashman KV, Sparks RSJ, Blundy JD (2017) Vertically extensive and unstable magmatic systems: a unified view of igneous processes. Science 355:eaag3055

Churikova TG, Ivanov BV, Eichelberger J, *et al.* (2013) Major and trace element zoning in plagioclase from Kizimen Volcano (Kamchatka): Insights into magma-chamber processes. *J Volcanol Seismol*, **7**, 112–130.

Erdmann S, Martel C, Pichavant M, Kushnir A (2014) Amphibole as an archivist of magmatic crystallization conditions: problems, potential, and implications for inferring magma storage prior to the paroxysmal 2010 eruption of Mount Merapi, Indonesia. *Contrib Mineral Petrol*, **167**, 1016.

https://doi.org/10.1007/s00410-014-1016-4

Feineman M, Moriguti T, Yokoyama T, *et al.* (2013) Sediment-enriched adakitic magmas from the Daisen volcanic field, Southwest Japan. *Geochem Geophys Geosystems*, **14**, 3009–3031.

Glazner AF, Bartley JM, Coleman DS, *et al.* (2004) Are plutons assembled over millions of years by amalgamation from small magma chambers? *GSA Today*, **14**, 4–12.

Kimura J-I, Gill JB, Kunikiyo T, *et al.* (2014) Diverse magmatic effects of subducting a hot slab in SW Japan: Results from forward modeling. *Geochem Geophys Geosystems*, **15**, 691–739.

Kimura J-I, Tateno M, Osaka I (2005) Geology and geochemistry of Karasugasen lava dome, Daisen–Hiruzen volcano group, southwest Japan. *Isl Arc*, **14**, 115–136.

Lange RA, Frey HM, Hector J (2009) A thermodynamic model for the plagioclase-liquid hygrometer/thermometer. *Am Mineral*, **94**, 494–506. https://doi.org/10.2138/am.2009.3011

Leake BE, Woolley AR, Arps CE, *et al.* (1997) Report. Nomenclature of Amphiboles: Report of the Subcommittee on Amphiboles of the International Mineralogical Association Commission on New Minerals and Mineral Names. *Mineral Mag*, **61**, 295–321.

Lepage LD (2003) ILMAT: an Excel worksheet for ilmenite–magnetite geothermometry and geobarometry. *Comput Geosci*, **29**, 673–678.

Morris PA (1995) Slab melting as an explanation of Quaternary volcanism and aseismicity in southwest Japan. *Geology*, **23**, 395–398. https://doi.org/10.1130/0091-7613(1995)023<0395:SMAAEO>2.3.CO;2

Nakagawa M, Hiraga N, Furukawa R (2011) Formation of a zoned magma chamber and its temporal evolution during the historic eruptive activity of Tarumai Volcano, Japan: Petrological implications for a long-term forecast of eruptive activity of an active volcano. *J Volcanol Geotherm Res*., **205**, 1–16. https://doi.org/10.1016/j.jvolgeores.2011.05.003

Nakagawa M, Wada K, Thordarson T, *et al.* (1999) Petrologic investigations of the 1995 and 1996 eruptions of Ruapehu volcano, New Zealand: formation of discrete and small magma pockets and their intermittent discharge. *Bull Volcanol*, **61**, 15–31.

Okada S, Ishiga S (2000) Tephras from Daisen Volcano. In: Field Guide of the 107th Annual Meeting of the Geological Society of Japan, pp. 81e90 (in Japanese)

Pineda-Velasco I, Kitagawa H, Nguyen T-T, *et al.* (2018) Production of high-Sr andesite and dacite magmas by melting of subducting oceanic lithosphere at propagating slab tears. *J Geophys Res Solid Earth*, **123**, 3698–3728.

Putirka KD (2008) Thermometers and Barometers for Volcanic Systems. In: Putirka KD, Tepley FJ (eds) Minerals, Inclusions and Volcanic Processes. *Mineralogical Soc Amer, Chantilly*, pp 61–120.

Ridolfi F, Renzulli A, Puerini M (2010) Stability and chemical equilibrium of amphibole in calc-alkaline magmas: an overview, new thermobarometric formulations and application to subduction-related volcanoes. *Contrib Mineral Petrol*, **160**, 45–66. https://doi.org/10.1007/s00410-009-0465-7

Smith VC, Staff RA, Blockley SP, *et al.* (2013) Identification and correlation of visible tephras in the Lake Suigetsu SG06 sedimentary archive, Japan: chronostratigraphic markers for synchronising of east Asian/west Pacific palaeoclimatic records across the last 150 ka. *Quat Sci Rev*, **67**, 121–137.

Sparks RSJ, Cashman KV (2017) Dynamic Magma Systems: Implications for Forecasting Volcanic Activity. *Elements*, **13**, 35–40.

Sparks RSJ, Young SR (2002) The eruption of Soufriere Hills Volcano, Montserrat (1995-1999): overview of scientific results. *Geol Soc Lond Mem*, **21**, 45–69.

Tamura Y, Yuhara M, Ishii T (2000) Primary Arc Basalts from Daisen Volcano, Japan: Equilibrium Crystal Fractionation versus Disequilibrium Fractionation during Supercooling. *J Petrol*, **41**, 431–448. https://doi.org/10.1093/petrology/41.3.431

Tamura Y, Yuhara M, Ishii T, *et al.* (2003) Andesites and dacites from Daisen volcano, Japan: partial-to-total remelting of an andesite magma body. *J Petrol*, **44**, 2243–2260.

Tsukui M (1984) Geology of Daisen Volcano. *J Geol Soc Jpn*, **90**, 643–658. https://doi.org/10.5575/geosoc.90.643

Tsukui M (1985) Temporal variation in chemical composition of phenocrysts and magmatic temperature at Daisen volcano, southwest Japan. *J Volcanol Geotherm Res*., **26**, 317–336.

Yamamoto T (2017) Quantitative eruption history of Pleistocene Daisen volcano, SW Japan. *Bull Geol Surv Jpn*, **68**, 1–16.

Yamamoto T, Hoang N (2019) Geochemical variations of the Quaternary Daisen adakites, Southwest Japan, controlled by magma production rate. *Lithos*, **350**, 105214

Zellmer GF, Iizuka Y, Miyoshi M, *et al.* (2012) Lower crustal H_2O controls on the formation of adakitic melts. *Geology*, **40**, 487–490.

(Received: Feb. 20, 2020, Accepted: Feb. 28, 2020)

（要　旨）

伊藤　豊・Andreas Auer，2020．烏ヶ山溶岩ドームおよびそれに関連する火砕流堆積物の岩石学的・鉱物化学的研究．島根大学地球科学研究報告，37，1-10

烏ヶ山溶岩ドームは大山－蒜山火山群の一部であり，その噴出物のほとんどはブロックとアッシュから構成される．火山噴出物は直接的に姶良－丹沢降下火砕物（AT）を覆い，その多くは大山の南側や南西側の主要な三つの谷を埋めるように流れ込み堆積した．アダカイト特性を有するデイサイト質マグマは，深さ 4 km から 12 km の間で結晶化する浅い地殻内の大きなマグマ溜まりから供給され，温度 803-920℃で，NNO バッファーでは Δlog+1.7 から +1.8 の酸素フガシティを示す．マグネシウムに富む斜方輝石斑晶のコアは，本質岩であるデイサイトと平衡状態ではなく，大山火山体の下にある巨大なマグマ溜まりからの苦鉄質補充を示す希少性の高い証拠である可能性がある．